International Journal on Recent and Innovation Trends in Computing and Communication ISSN: 2321-8169
Volume: 3 Issue: 11 6194 - 6199

Nanostructured CdO doped MnO_2 Thick Film Resistors as Ethanol Sensors

R. R. Attarde, D. R. Patil*
Bulk and Nanomaterials Research Laboratory,
Dept. of Physics, R. L. College, Parola,
Dist. Jalgaon, MHS, India, 425111
E-mail: prof_drpatil@yahoo.in Mob: +91 9860335029

Abstract- The disc type ultrasonicated microwave assisted centrifuge technique was used for the synthesis of nanostructured pure and CdO doped MnO_2 powders. The dry powders of as synthesized materials were transformed into thick films by screen printing technique. Synthesized stoichiometric pure MnO_2 was observed to be less sensitive to hazardous, toxic and inflammable gases, though they are of nanoscaled. Doping of CdO in MnO_2 results in enhancing the gas sensing performance to ethanol. It was observed that, the ethanol response of 3 wt% CdO doped MnO_2 thick films, increase crucially at 250^{o}C. It was also observed that, further increase in doping concentration would leads to decrease the gas response. Various characterization techniques were employed to study the surface morphology, structure of the crystal, phases, particle's size, etc. Effect of the surface nanostructure, different gases, gas concentrations, particle size, long duration for ageing, etc. on the gas response of the samples were studied and discussed. The quick response and fast recovery are the main features of this sensor.

Keywords: *CdO doped MnO_2, Thick films, Ethanol gas sensors, etc.*

*****

I. INTRODUCTION

Semiconducting oxides such as ZnO, SnO_2, Fe_2O_3, Cr_2O_3, etc. [1-8] are widely used as inexpensive sensors for monitoring polluting and combustible gases and vapors in safety and automotive applications. However, MnO_2 is attracting considerable attention for its large applicability in many fields, easy availability in abundant and at low cost. Very few reports are available on MnO_2 in the field of gas sensing. In fact pure MnO_2 thick films were reported to have poor gas sensitivity.

Ethanol is explosively utilized for beverages, industrial and scientific applications. Ethanol is a hypnotic [9, 10] (sleep producer) and toxic [10-13] in nature. Heavy exposure or consumption of beverages increases the risk of hazards of cancer [14] of the upper respiratory and digestive tracks, liver, breasts (in case of women), etc. Workers working for the ethanol synthesis have great chances of being victim of respiratory and digestive track cancer. It depresses the activity in the upper brain even though it gives the illusion of being a stimulant. Abuse of ethanol is a major drug problem in most of the countries. The gas sensing performances of pure semiconducting materials in the form of thick films [15-21] can be improved by incorporating few additives into the base material and / or surface activation [22, 23] of thick films.

Few sensor models are also available for detecting ethanol vapors. However, some limitations are still persists with them. To detect the ethanol vapors below threshold limit value, to reduce the cost, to increase the applicability of the sensors, to make available the sensor models to laymen in the affordable cost, to make the sensor models in portable size for easily transport, etc. it is necessary to develop the ethanol gas sensors for smart applications.

The aim of the present work is to develop the low cost, highly applicable, quick response, fast recovery, highly sensitive, highly selective gas sensors by modifying MnO_2 thick films, which could be able to detect the C_2H_5OH gas at trace levels, i. e. below Threshold Limit Value (TLV).

II. EXPERIMENTAL SECTION

A. Synthesis of pure and CdO doped MnO_2 powders

Nanostructured pure MnO_2 and CdO doped MnO_2 powders were synthesized by disc type ultrasonicated microwave assisted centrifuge technique, by hydrolysis of AR grade manganese chloride in aqueous-alcohol solution. An initial aqueous-alcohol solution was prepared from distilled water and propylene glycol in the ratio of 1:1. This solution was then mixed with aqueous solution of manganese chloride and cadmium chloride (dopant in the proportion 1, 3, 5 and 7 wt%) in the ratio such that the elemental concentration was 0.1M and the alcohol to water ratio was 1:1. The special arrangement was made to add drop wise aqueous ammonia (0.1ml / min.) with constant stirring till the optimal pH of solution becomes 8.3. After complete precipitation, the hydroxide was washed with distilled water until chloride ions were not detected by $AgNO_3$ solution. Then the hydroxide in a glass beaker was placed in a microwave oven for 15 minutes with on-off cycles, periodically. The dried precipitate was ground by agate pestle-mortar and annealed in a muffle furnace at 600°C for 3h. The phase purity and degree of crystallinity of MnO_2 powder were monitored by XRD analysis.

B. Thick film fabrication

The ultrafine powders of pure MnO_2 and CdO doped MnO_2 were calcined at 600^{0}C for 3 h in air and reground to ensure sufficiently fine particle size. The thixotropic pastes [16-21] were formulated by mixing the synthesized nanostructured powders of pure and CdO doped MnO_2 (one at a time) with a solution of ethyl cellulose (a temporary binder) in a mixture of organic solvents such as butyl cellulose, butyl carbitol acetate and turpineol. The ratio of inorganic to organic part was kept as 80: 20 in formulating the pastes. The thixotropic pastes were screen printed on the

glass substrates in desired patterns. The actual size of the film printed on glass substrate is 9 mm x 4 mm. These films prepared were dried at 80°C under an IR lamp, followed by firing at 500°C for 30 min in ambient air. Silver contacts were made by vacuum system. These films are now ready to use as the ethanol gas sensing elements in the static gas sensing system.

C. Details of static gas sensing system

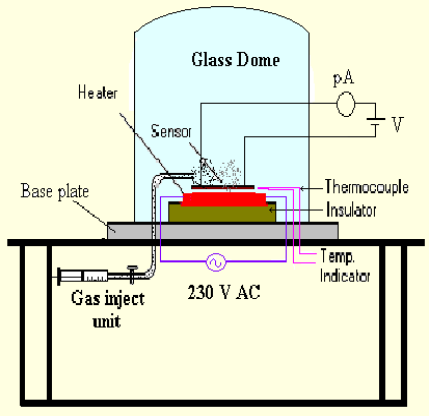

Fig. 1: Block diagram of static gas sensing system

Fig. 1 represents static gas sensing system [10] to examine the sensing performance of the thick films. There were electrical feeds through the base plate. The heater was fixed on the base plate to heat the sample under test upto required operating temperature. The current passing through the heating element was monitored using a relay with adjustable ON and OFF time intervals. A Cr-Al thermocouple was used to sense the operating temperature of the sensor. The output of the thermocouple was connected to a digital temperature indicator. A gas inlet valve was fitted at one of the ports of the base plate. The required gas concentration inside the static system was achieved by injecting a known volume of test gas using a gas-injecting syringe. A constant voltage was applied to the sensor, and current was measured by a digital pico-ammeter. Air was allowed to pass into the glass dome after every ethanol gas exposure cycle.

III. MATERIAL CHARACTERIZATIONS

A. Structural properties (X-Ray Diffractogram)

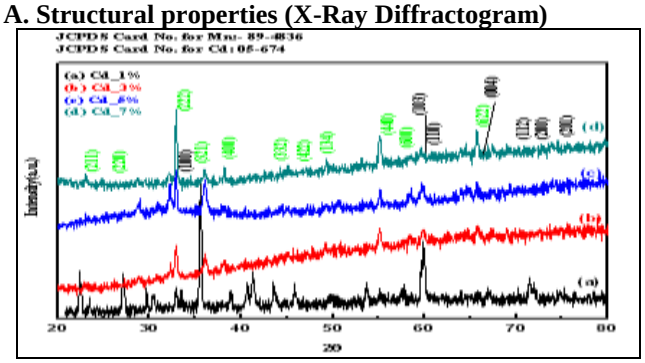

Fig.2: XRDs of CdO doped MnO_2 powders

X ray diffraction study of CdO doped MnO_2 powders was carried out using BRUKER AXSD8 (Germany) advanced model X ray diffraction with $CuK\alpha_1$ (λ=1.54056 Å) radiation in the 2θ range 20^0-80^0. The scanning speed of the specimen was maintained 0.5^0 /min. Fig. 2 depicts the XRD of CdO doped MnO_2 powders. The 2θ peak observed at 22.96, 26.2, 33.45, 35.25, 38.22, 44.28, 48.84, 50.30, 56.21, 59.23 and 66.55 which correspond to the (211), (220), (222), (321), (400), (332), (422), (134), (440), (600) and (622) planes of reflections. The XRD spectrum reveals that the materials are polycrystalline in nature and hexagonal in structure. The observed peaks are matching well with ASTM reported data of pure MnO_2. The material was observed to be nanocrystalline in nature. There are no prominent peaks of CdO associated in XRD pattern of MnO_2 due to smaller wt % of CdO in comparison with MnO_2. The lattice parameters were found to be a = 3.5817 and c = 5.6659. The unit cell volume was evaluated as 62.95. The average grain size was determined using Scherer's formula.

Table 1: Crystallinity and amorphous nature of as synthesized powders

Material	Doping (%)	Crystallinity (%)	Amorphous (%)
Pure MnO_2	0	32.4	67.6
CdO doped MnO_2	1	42.4	57.6
	3	45.6	54.4
	5	50.7	49.3
	7	58.6	41.4

It was also observed from XRD analysis that, the as synthesized pure MnO_2 powder has more amorphous nature (67.6%) and less crystallinity (32.4%). However, the amorphous nature decreases (i. e. crystalline nature increases) with the percentage of doping with cadmium oxide (Table 1). This may be attributed to the fact that, on doping, cadmium reacts and makes tight binding with the manganese which would require more ultrasonic power to make the powder amorphous.

B. Scanning Electron Microscopic Studies (Microstructural analysis)

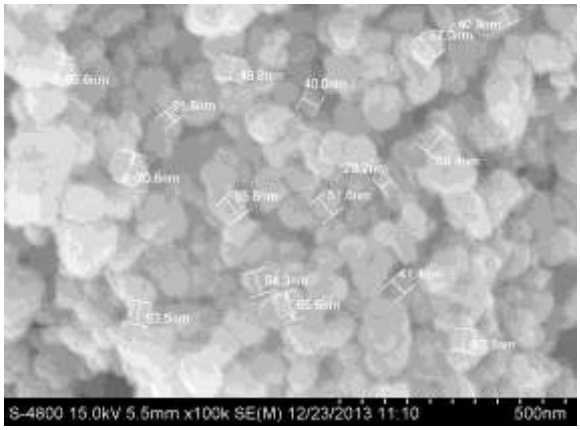

(a) Unmodified (pure) MnO_2 film

 ISSN: 2321-8169
6194 - 6199

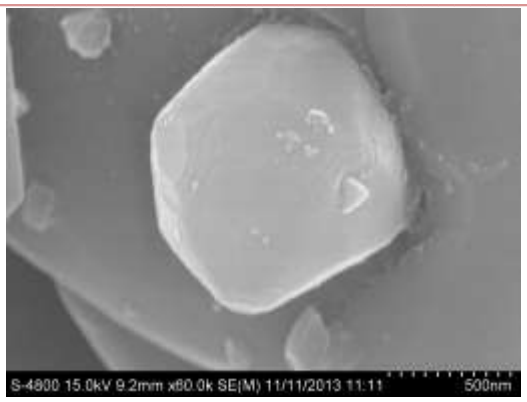

(b) CdO doped MnO_2 film (1 wt%)

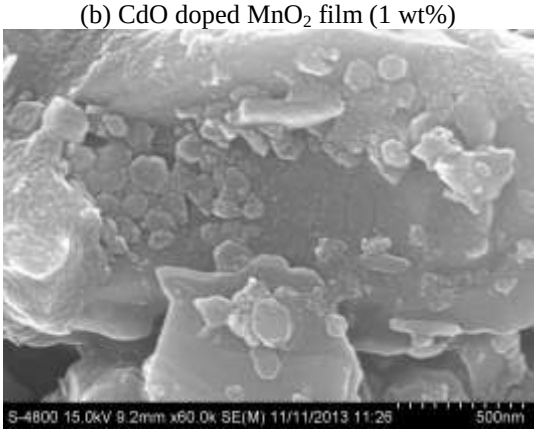

(C) CdO doped MnO_2 film (3 wt%)

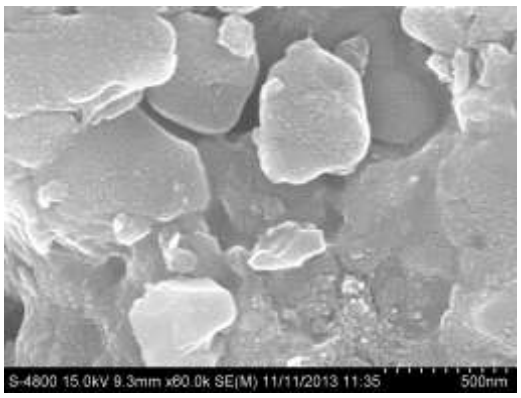

(d) CdO doped MnO_2 film (5 wt%)

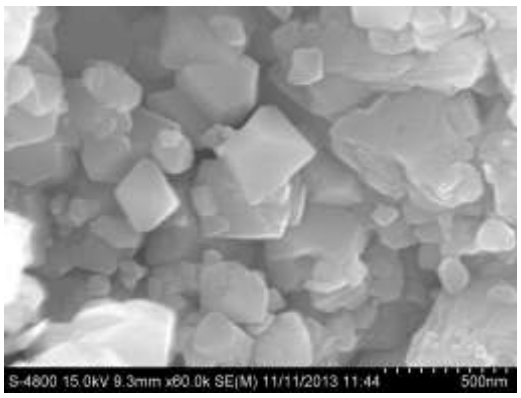

(e) CdO doped MnO_2 film (7 wt%)

Fig. 3: SEM images of nanostructured CdO doped MnO_2 films

Fig. 3 (a) depicts the SEM image of an unmodified (pure) MnO_2 thick film fired at 500^0C for 30 min. Unmodified MnO_2 film consists of voids and a wide range of randomly distributed grains with grain sizes ranging from 30 nm to 50 nm distributed as lumps. Fig. 3 (b) depicts the microstructure of CdO (1 wt %) doped MnO_2 film consisting of smaller grains of CdO associated with the larger grains of MnO_2. The larger grains of MnO_2 occurred due to agglomeration of its smaller grains. The film consists of island like structure and grains with sizes ranging from 20 nm to 1100 nm distributed non-uniformly. Fig. 3 (c) depicts the microstructure of CdO (3 wt %) doped MnO_2 film, which consists large number of grains of CdO associated with the grains of MnO_2 as compared to that in Fig. 3 (b). The film consists of voids and a wide range of grains with grain sizes ranging from 20 nm to 1000 nm distributed non-uniformly. Fig. 3 (d) depicts the microstructure of CdO (5 wt %) doped MnO_2 film consisting of even smaller grains of CdO in association with MnO_2 as compared to that in Figs. 3 (b and c). The most of the grains of MnO_2 are covered with smaller grains of CdO. The films consist of voids and a wide range of grains with grain sizes ranging from 10 nm to 900 nm distributed non-uniformly. Fig. 3 (e) depicts the microstructure of CdO (7 wt %) doped MnO_2 film consisting of smaller grains of CdO in association with larger grains of MnO_2. The grains of MnO_2 are having octahedral shape and size and oriented randomly. However, the grains of CdO are random in nature. The film consists of voids and a wide range of grains with grain sizes ranging from 10 nm to 500 nm distributed non-uniformly.

IV. ELECTRICAL BEHAVIOUR

A. I-V Characteristics of the films

Fig. 4 depicts the I-V characteristics of pure and CdO doped MnO_2 films. It is clear from the symmetrical nature of I-V characteristics that, the materials as well as silver contacts made on the films are ohmic in nature. The material is therefore said to have resistive properties.

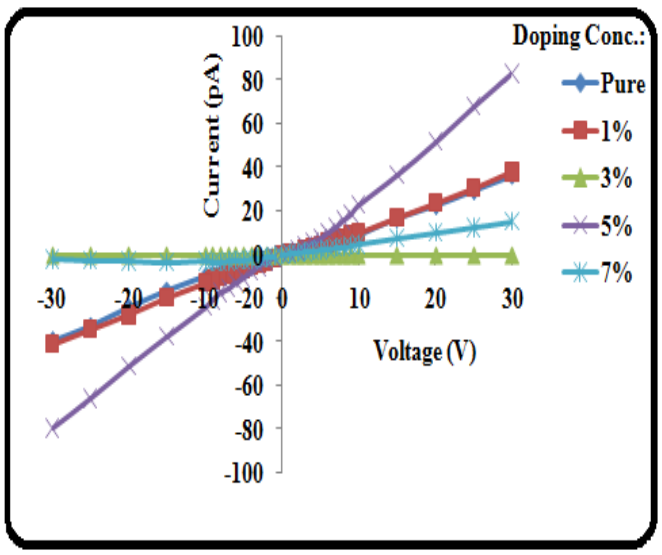

Fig. 4: I-V Characteristics of CdO doped MnO_2 films

 ISSN: 2321-8169
6194 - 6199

B. Conductivity-Temperature dependence

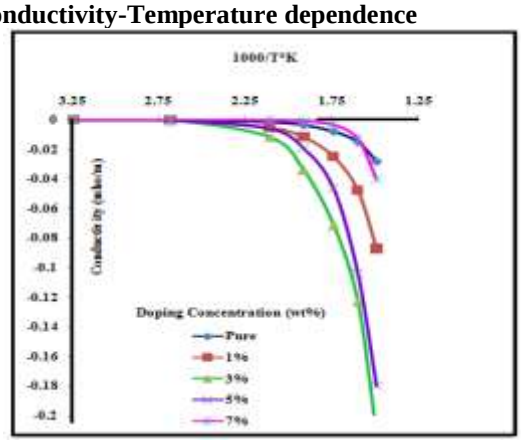

Fig. 5: Conductivity-Temperature profile of CdO doped MnO_2 films

Fig. 5 shows the variation of conductivity with the reciprocal of operating temperature. The conductivities of all samples are decreasing with increase in operating temperature. The decrease in conductivity with increase in temperature could be attributed to positive temperature coefficient of resistance and hence the semiconducting nature of the CdO modified MnO_2 samples.

V. GAS SENSING PERFORMANCE

A. Measurement of gas response, selectivity, response and recovery time

Response of the sensor for the particular gas can be defined as the ratio of the change of conductance of the sample upon exposure to the gas to the conductance in air ambient. The gas response (S) can be written as:

$$\text{Gas response} = \frac{G_g - G_a}{G_a} = \frac{\triangle G}{G_a}$$

where G_a = conductance in air and G_g = conductance in a target gas.

Specificity or selectivity of the sensor can be defined as the ability of a sensor to respond to a particular gas in the mixture of various gases. Response time (RST) is defined as the time required for a sensor to attain the 90% of the maximum increase in conductance after exposure of the test gas, while recovery time (RCT) is the time taken to get back 90% of the maximum conductance [10] in air.

B. Sensing performance of the sensor

B (i). Effect of operating temperature

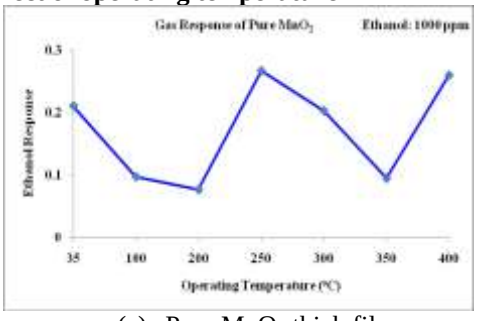

(a) Pure MnO_2 thick films

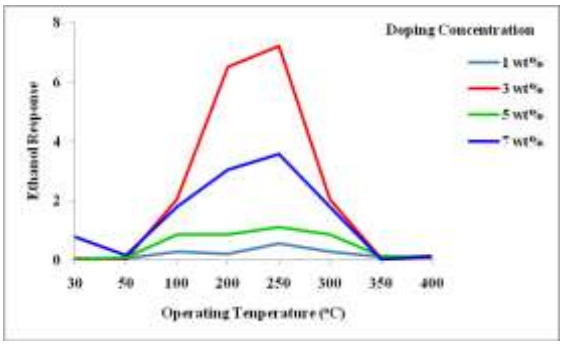

(b) CdO doped MnO_2 thick films

Fig. 6: Variation of Ethanol response with op. temperature

Fig. 6 (a) shows the variation of C_2H_5OH vapors (1000 ppm) response of pure MnO_2 with operating temperature. The lowest and random response for C_2H_5OH gas was observed as a function of operating temperature. The maximum response obtained is of the order of 0.27 at 250^0C. Also, it has least selectivity to ethanol gases against different gases. This is the major drawback of pure MnO_2 thick films. Fig. 6 (b) depicts the variation of gas response of CdO doped MnO_2 to ethanol vapors (50 ppm) with operating temperature. The largest response of CdO doped MnO_2 (3 wt %) to ethanol was observed at 250^0C. The response could be attributed to the adsorption-desorption type sensing mechanism. The number of oxygen adsorbed on the surface would depend on the number of CdO misfits on the MnO_2 surface and operating temperature. Response curve is having the lack of sharpness.

B (ii). Active region of the sensor

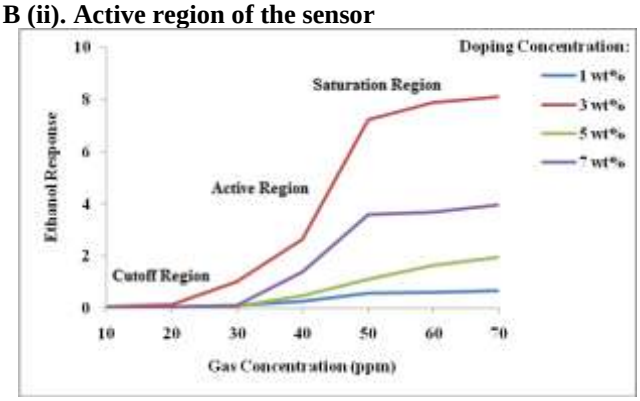

Fig. 7: Variation in response with Ethanol concentration (ppm)

The variation of gas responses of CdO-doped MnO_2 samples with ethanol vapor concentrations is depicted in Fig. 7. It has been observed from the figure that the gas responses go on increasing linearly with gas concentration up to 50 ppm. The rate of increase in response was relatively larger up to 50 ppm and saturated beyond 50 ppm. The monolayer of the gas molecules formed on the surface could cover the whole surface of the film. The gas molecules from that layer would reach the surface active sites of the film. The excess gas molecules lying above the monolayer formed on the surface would remain idle and would not

reach the surface active sites of the sensor. So, the gas response at higher concentrations of the gas is not expected to increase further, in the proportion. Thus, the active region of the sensor would be up to 50 ppm. For proper functioning of the sensor, one should work in the active region only.

B (iii). Effect of doping concentration

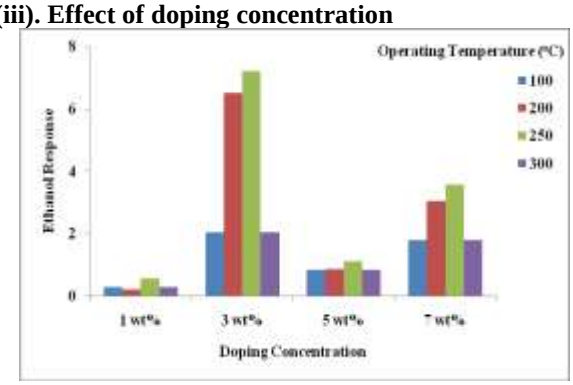

Fig. 8: Variation of Ethanol response with doping concentration (wt%)

It is clear from the observations that, the change in doping concentrations in wt % of CdO into MnO_2 changes the sensing habits and therefore it may sense different gases at different level of doping. Fig. 8 indicates the C_2H_5OH gas response as a function of the amount (wt %) of CdO doped in MnO_2. CdO (3 wt %) doped MnO_2 sample was observed to be the most sensitive to ethanol at 250^0C. The higher response to ethanol vapors (50 ppm) may be attributed to the optimum porosity and largest effective surface area available to react the gas molecules and appropriate number of CdO misfits to adsorb the oxygen which in turn would oxidize the exposed gas.

B (iv). Selective nature of the sensor

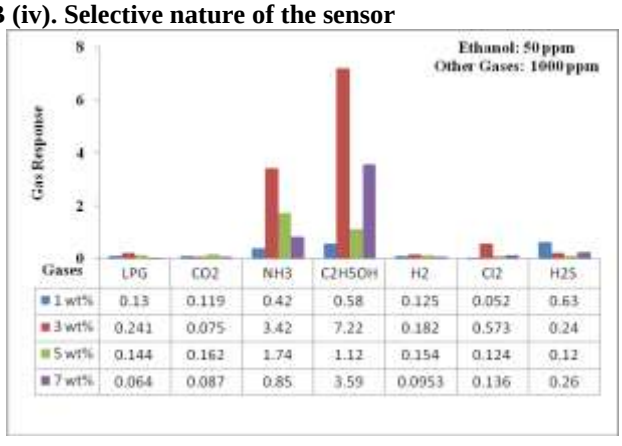

Gases	LPG	CO2	NH3	C2H5OH	H2	Cl2	H2S
1 wt%	0.13	0.119	0.42	0.58	0.125	0.052	0.63
3 wt%	0.241	0.075	3.42	7.22	0.182	0.573	0.24
5 wt%	0.144	0.162	1.74	1.12	0.154	0.124	0.12
7 wt%	0.064	0.087	0.85	3.59	0.0953	0.136	0.26

Fig. 9: Selectivity of Ethanol vapors among various gases

It is observed from Fig. 9 that the CdO doped (3 wt %) MnO_2 sensor gives maximum response to ethanol vapors (50 ppm) at 250^0C. The sensors showed highest selectivity for ethanol among all other tested gases viz. LPG, CO_2, H_2S, H_2 and Cl_2. However, it has least selectivity with respect to NH_3.

VI. DISCUSSION

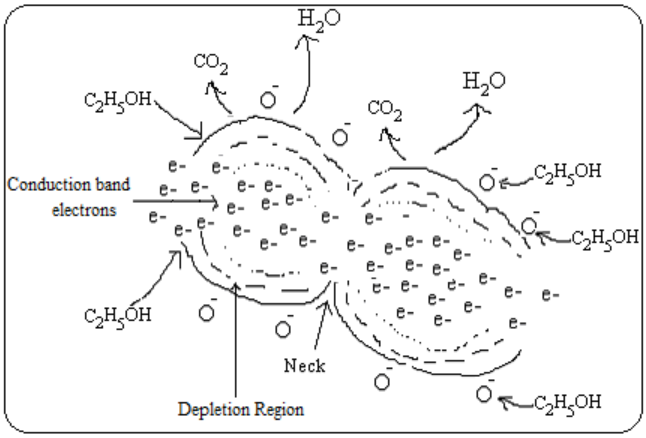

Fig. 10: Mechanism of Ethanol gas sensing

The atmospheric oxygen molecules O_2 are adsorbed [10] on the surface of the thick film (Fig. 10). They capture the electrons from conduction band [Eq. 1] from the bulk of the material as follows:

$$O_{2\,(air)} + 2e^- \rightarrow 2O^-_{(film\ surface)} \quad \ldots\ldots\ldots\ldots 1$$

This results in decrease in electronic conductivity of the material of the film. The mass % of Mn and O in each samples were not as per the stoichiometric proportion and all samples were observed to be oxygen deficient. This deficiency gets reduced (though in less extent) due to adsorption of atmospheric molecular oxygen. This helps in decrease in electronic conductivity of the film. Upon exposure, ethanol vapor molecules got oxidized with the physisorbed oxygen species producing CO_2 and H_2O [Eq. 2]. This results in evolving oxygen as electrically neutral atoms trapping behind the electrons in the material. The activation energy is the minimum energy required to activate the material, so that, the material responds to a particular gas. Activation energy decreases with increase in temperature in air ambient. It means that least energy is required to activate the material at high temperature. Also, activation energy increases with operating temperature in gaseous medium. It means that large energy is acquired by the electrons during exposure of ethanol. Upon exposure of ethanol gas, the energy released in decomposition of ethanol molecules, would be sufficient for trapped electrons to jump into the conduction band of modified MnO_2; resulting in increase in the conductivity of the thick film of modified MnO_2. When ethanol reacts with oxygen, a complex series of reactions take place, converting ethanol vapors to carbon dioxide and water as:

$$\mathbf{C_2H_5OH_{(gas)} + 6O^-_{film\ surface)} \rightarrow 2CO_{2\,(gas)} + 3H_2O_{(gas)} + 6e^-_{cond.band)} \ldots 2}$$

This shows n-type conduction mechanism. Thus on oxidation, single molecule of ethanol liberates six electrons [eq. 2] in conduction band, results in increase in conductivity of the sensor. Increase in operating temperature causes oxidation of large number of ethanol molecules, thus producing very large number of electrons. Therefore conductivity increases in large extent. This is the reason,

why the gas response increases with operating temperature. The thermal energy (temperature) at which the gas response is maximum, is the actual thermal energy needed to activate the material for progress in reaction. However, the response decreases at higher operating temperature, as the oxygen adsorbates are desorbed from the surface of the sensor. Also, at higher temperature, the carrier concentration increases due to intrinsic thermal excitation and the Debye length decreases. This may be one of the reasons for decreased gas response at higher temperature.

VII. CONCLUSIONS

1. Pure stoichiometric MnO_2 thick films were observed to be less sensitive to trace level of ethanol vapors.
2. The CdO doped (3 wt%) MnO_2 thick film sensor was found to be highly selective to ethanol vapors (50 ppm) in the mixture of various gases of higher concentrations (1000 ppm).
3. The sensor showed quick response and fast recovery.

ACKNOWLEDGEMENTS

Authors are grateful to Hon'ble Kakasaheb Vasantrao More, President and Prin. B. V. Patil, Rani Laxmibai College, Parola, Maharashtra, India for providing excellent laboratory facilities, at Bulk and Nanomaterials Research Laboratory, Dept. of Physics, R. L. College, Parola, Dist-Jalgaon, MHS, India.

REFERENCES

[1] T. Seiyama, A. Kato, K. Fujitshi, M. Nagatanui, Anal. Chem., 34 (1962) 1502.
[2] P. T. Moseley, Sens Actuators B 6 (1992) 149-156.
[3] L. A. Patil, D. R. Patil, Heterocontact type CuO-modified SnO_2 sensor for the detection of a ppm level H_2S gas at room temperature, Sens. Actuators B 120 (2006) 316-323.
[4] D. R. Patil, L. A. Patil, G. H. Jain, M. S. Wagh, S. A. Patil, Surface activated ZnO thick film resistors for LPG gas sensing, Sens. Transducers 74 (2006) 874-883.
[5] G. H. Jain, L. A. Patil, M. S. Wagh, D. R. Patil, S. A. Patil, D. P. Amalnerkar, Surface modified $BaTiO_3$ thick film resistors as H_2S gas sensors, Sens. Actuators B 117 (2006) 159-165.
[6] M. S. Wagh, G. H. Jain, D. R. Patil, S. A. Patil, L. A. Patil, Surface customization of SnO_2 thick films using RuO_2 as a surfactant for the LPG response, Sens. Actuators B 122 (2007) 357-364.
[7] S. A. Patil, L. A. Patil, D. R. Patil, G. H. Jain, M. S. Wagh, CuO-modified tin titanate thick film resistors as H_2-sensors, Sens. Actuators B 123 (2007) 233 - 239.
[8] D. R. Patil, L. A. Patil, Room temperature chlorine gas sensing using surface modified ZnO thick film resistors, Sens. Actuators B 123 (2007) 546-553.
[9] T. W. Graham Solomans, C. B. Fryhle, Organic Chemistry, (8th ed.), John Wiley and Sons Inc., (2004) 497- 498.
[10] D. R. Patil, Ph. D. Thesis (2007).
[11] D. R. Patil, L. A. Patil, D. P. Amalnerkar, Ethanol gas sensing properties of Al_2O_3-doped ZnO thick film resistors, Bull. Mater. Sci.-Springer link 30 (2007) 553-559.
[12] S. D. Kapse, F. C. Raghuwanshi, V. D. Kapse, D. R. Patil, Characteristics of high sensitivity ethanol gas sensors based on nanostructured spinel $Zn_{1-x}Co_xAl_2O_4$, J. Current Appl. Phys. 12 (2012) 307 – 312.
[13] G. S. Sodhi, Fundamental concepts of Environmental Chemistry, (1st edition), Narosa Publishing House, New Delhi, (2002) pp 135.
[14] R. A. Michaels, Environ. Health Perspective, 107 (1999) 617-627.
[15] D. R. Patil, Ph. D. Thesis (2007), Chapter 4, pp. 105 – 131.
[16] D. R. Patil, L. A. Patil, Preparation and study of NH_3 gas sensing behavior of Fe_2O_3 doped ZnO thick film resistors, Sens. Transducers 70 (2006) 661-670.
[17] D. R. Patil, L. A. Patil, P. P. Patil, Cr_2O_3-activated ZnO thick film resistors for ammonia gas sensing operable at room temperature, Sens. Actuators B 126 (2007) 368–374.
[18] D. R. Patil, L. A. Patil, Ammonia sensing resistors based on Fe_2O_3-modified ZnO thick films, Sensors IEEE 7 (2007) 434-439.
[19] U. B. Gawas, V. M. S. Verenkar, D. R. Patil, Nanostructured ferrite based electronic nose sensitive to ammonia at room temperature, Sens. Transducers 134 (2011) 45-55.
[20] K. A. Khamkar, S. V. Bangale, V. V. Dhapte, D. R. Patil, S. R. Bamne, A Novel Combustion Route for the Preparation of Nanocrystalline $LaAlO_3$ Oxide Based Electronic Nose Sensitive to NH_3 at Room Temperature, Sens. Transducers 146 (2012) pp. 145-155.
[21] M. S. Shinde, D. R. Patil, R. S. Patil, Ammonia gas sensing property of nanocrystalline Cu_2S thin films, I. J. Pure and Applied Physics, 51, (2013) pp 713-716.
[22] C. Xiangfeng, L. Xingqin, M. Guangyao, Sens. Actuators B 65 (2000) 64-67.
[23] S. Matsushima, T. Maekawa, J. Tamaki, N. Miura, N. Yamazoe, Chem. Lett. (1989) 845-848.
[24] D. R. Patil, Need of gas sensors, J. Everyman's Science, 46 (2011) pp. 155 – 161.
[25] S. V. Bangale, S. M. Khetre, D. R. Patil, S. R. Bamne, Sens. Transducers 134 (2011) 95-106.